Journal of the Persian Gulf
(Marine Science)/Vol. 7/No. 23,24/ March & June 2016/10/79-88

Study of Current Profile in the Khuran Channel using ADCP Measurements

Khosravi, Maziar[1*]; Chegini, Vahid[1]; Siadat Mosavi, Seyed Mostafa[2]; Vennell, Ross[3]

1- Iranian National Institute for Oceanography and Atmospheric Science, Tehran, IR Iran

2- School of Civil Engineering, Iran University of Science and Technology, Tehran, IR Iran

3- Dept. of Marine Science, University of Otago Dunedin, New Zealand

Received: May 2016 *Accepted: August 2016*

Abstract

Thirteen repetitions of a cross-channel transect in the Khuran Channel within the Strait of Hormuz allowed the description of the mean flow and semidiurnal tidal properties of a north-south transect. Water velocity profiles were obtained with a 614.4 kHz TRDI Work Horse Broadband ADCP along this 3.3 km long transect on 10 October 2014, the third day of secondary spring tide. The M2, M4 and M6 frequencies were separated from the observed current using sinusoidal least squares regression analysis. The semidiurnal tidal currents along this transect exhibited typical amplitudes of 160-170cm/s, decreasing toward coastal waters. The mean flow which confirmed the occurrence of asymmetry between ebb and flood phase of tidal current in Khuran Channel were ebb dominant in the deeper part of the channel and southern slopes and flood dominant over the shallower areas, with greatest magnitudes (10 cm/s) near the surface mainly in the deeper parts of the northern side of the channel. The tidal current amplitudes decreased and for the most with depth and followed the bathymetry particularly in the middle of channel, which reveals the dominants of frictional forces. The large overtide amplitude is as a result of nonlinearities that were produced by increased frictional effects that lead to the asymmetry between ebb and flood phase of tidal current in this channel.

Keywords*: Khuran Channel, Strait of Hormuz, Tidal Currents, Persian Gulf*

1. Introduction

Moving vessel ADCP surveys have long been employed to measure velocity profiles in many applications (e.g., (Geyer and Signell 1990, Münchow, Garvine et al. 1992, Valle-Levinson and Lwiza 1997, Old and Vennell 2001, Cáceres, Valle-Levinson et al. 2003, Carpman and Leijon 2014, Chen, Wang et al. 2016, Buschman 2017)). Studies of (Münchow, Garvine et al. 1992) and (Geyer and Signell 1990) compared the performance of moving vessel ADCPs with data collected by moored current meters and found a fair agreement between both, although they observed random noise in the velocity measurements of between 0.03 and 0.07 m/s, which Munchow et al. (1992) found to be correlated with the sea state and removed the noise through spatial and temporal averaging. Also the study of (Cáceres, Valle-Levinson et al. 2003) employed moving vessel ADCP survey to observe the transverse dynamics of flow in a highly energetic tidal channel (Chacao channel) and found

* *E-mail: mazyar. khosravi@inio.ac.ir*

that the mean flow is flood dominated at all depths in shallow areas and ebb dominated in deeper areas of the same cross section.

In fact, a moving vessel ADCP records vertical profiles of velocity vectors from the surface along a series of vertical bins. The ADCP is mounted on one side of a moving vessel with its transducers placed just below the surface and facing downward. Discrete velocity data are measured in a series of vertical ‘‘bins.’’ The first valid bin is away from the transducer by a distance determined by the userdefined vertical bin size, the speed of sound, and the ‘‘blanking distance’’. The data near the bottom within a thin layer of the water column are invalid due to the ‘‘sidelobe’’ interference and need to be discarded.

Overtide is a secondary tide of higher frequency than the principal tide (e.g. M_4, M_6, …). Overtides have periods that are an exact multiple of the fundamental constituents, e.g. M_4, a multiple of M_2, have a period of 6.21 hrs and also M_6, a triple of M_2, have a period of 4.14 hrs (see table 1). The generation of overtides is one of the dominant nonlinear physical processes in many coastal areas and tidal channels. It results from interactions between tidal flow and topography (Parker, 1991).

Table 1: Frequencies and periods of M2, M4 and M_6

Tide	Frequency (rad sec^{-1})	Period (h)
M_2	0.00014051892	12.42
M_4	0.00028103783	6.21
M_6	0.00042155675	4.14

In fact, overtides are harmonic motions with higher frequencies than the semidiurnal, may be generated by advection accelerations and bottom friction. They may produce flood/ebb asymmetries, which play a key role in the long-term distribution of sediments. The tidal-mean flow in a channel like Khuran channel may also be induced by nonlinear interactions of tidal flow with topography. The source terms for M_4 usually arise from the nonlinear terms of advection, continuity, and bottom friction; while the M_6 are generated mainly by terms from bottom friction. Overtides tides are detectable in the sea surface elevation and in the velocity fields (Aubrey and Speer 1985, Parker 1991).

In this study, we apply the method of Old and Vennell (Old and Vennell 2001) to the Khuran Channel (KCh) to obtain both mean flow and tidal velocity across the main channel within a 3.3 km long transect. We will use a sinusoidal least squares regression analysis described in (Cáceres, Valle-Levinson et al. 2003) to infer the M_2, M_4 and M6characteristics of the semidiurnal tidal constituents of observed current.

2. Study Area and Objective of the Study

The Straits of Hormuz is a key waterway which connects the Persian Gulf to the north part of the Indian Ocean. The KCh in the Strait of Hormuz located at 26°45’N and 55°40’E with ~110 km length and minimum width of 3.2 km at the port of Pol. The KCh is a topographically complex channel which is open at both ends.Owning to its particular geometry, this narrow channel is considered to being an area with strong tidal currents. Bathymetric maps by National Cartographic Center of Iran (NCC) show the maximum depth in this shallow channel reaches to 42 m in a trench at its narrowest section (Figure 1). Results of moored current meters measurements by (Azizpour et al. 2016) in the Strait of Hormuz showed that tidal currents have the main contributions in the observed current throughout the water column.

The tides in the Strait of Hormuz and then including in the KCh are co-oscillate those in the northern Indian Ocean (Reynolds 1993). The tidal current in the KCh is directed westward at the flood and eastward at the ebb. Previous moored current meter observations in the KCh by (Zaker, Ghaffari et al. 2011) shows that currents are dominated by tidal forcing with mixed semi-diurnal characteristics that the M2 is the largest tidal signal (the location of this mooring is appeared on the Fig. 1).

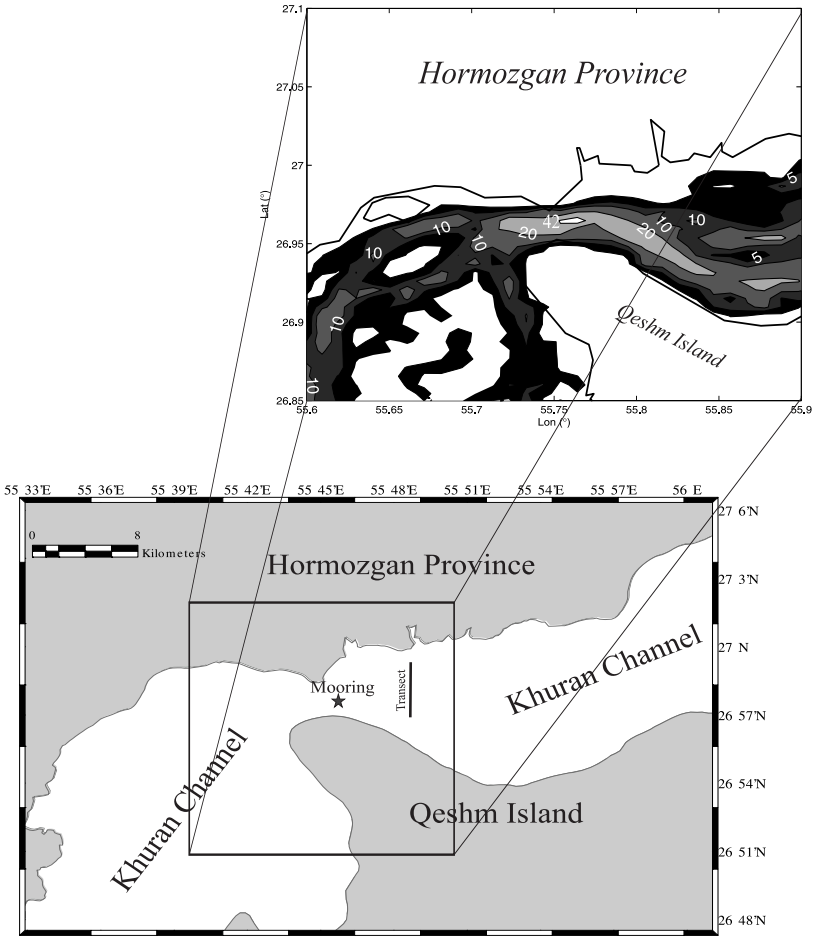

Fig. 1: Map of study area. The across-channel transect in this study was located at the right side of the narrowest section of KCh. The mooring location is shown at the narrowest section.

Also it was concluded that the water column over most of the KCh is almost vertically homogenous. Hence, that tides in this shallow channel are likely almost barotropic. Current data from that moored current meter measurements is also applied in this study (Fig 1). This mooring was deployed within the narrowest section during a period of 34 days in 5 meter below the water surface in the summer 2005 (Zaker, Ghaffari et al. 2011).

Direct current measurements in the KCh are terribly essential and meanwhile difficult to carry out. The high volume of ship traffic combined with extensive fishing activities make this region very risky for moored observations. Combing higher measurement accuracy of ADCPs with the convenient positioning system, it is possible to measure the spatial variations in the flows on the small spatial scales. Thus, moving vessel ADCP surveys allow the system dynamics to be estimated directly from the data instead of concluding them from fixed point current observations assuming some theoretical form (Old and Vennell 2001). The moving vessel-ADCP surveys that presented in this study have provided the description of the spatial variability of mean and tidal flow on a cross-channel transect within the KCh.

3. Materials and Methods

3.1. Measurement Setup

Observations were made on October 10, 2014, using a ~3m-long vessel. The tide was at the third day of secondary spring tide. There was no major wind event during the observations. A 614.4 kHz TRDI Work Horse Broadband ADCP with bottom tracking was mounted looking downward on the

starboard side of the vessel. The ADCP specification is provided in Table 2. The depth of the ADCP transducers was set to be ~0.83 m below the water surface. Considering that the blanking distances for this ADCP have to be 1m, hence the top of the first bin was ~1.83 m water depth. Furthermore, a Garmin GPSMAP 521s was used for the navigation and recording of the position. The ADCP was configured to sample 1-m vertical bins, and the data were averaged at 40-s intervals. A predefined transect with a total length of about 3.3 km was followed by the vessel repeatedly 15 times over a 13-hour period. The boat speed was maintained at about 5 knots (2.5 m/s) throughout the observations (see Fig. 2).

3.2. Data Analysis

The KCh is almost along the east-west axis, however, the Principle Component Analysis (PCA) revealed that the direction of greatest shear variability of the tidal currents and of weakest across-channel tidal flows was -5 degrees. Thus the data were rotated 5 degrees clockwise to east-west (x-direction, u-component) and north-south (y-direction, v-component) and ADCP ship`s error calibrate compass, as (Joyce 1989).

After rotation of the axes, the instantaneous data were adjusted into uniform grids of 1m depth and 100m length aligned with tracks and the analysis performed independently on the time series generated at each grid point. The M_2, M4 and M_6 frequencies were separated from the observed current using sinusoidal least squares regression analysis (Eq. 1):

$$u = u_0 + \sum a_n \cos(\omega_n - \Phi_n) \quad (1)$$

Table 2: Equipment Specification: Acoustic Doppler Current Profiler

Velocity Accuracy	Sentinel 600 KHz: ±2.5mm/s
Velocity Resolution	1 mm/s
Velocity Range	±5 m/s (default) and ± 20m/s (maximum)
Vertical Resolution (Long Range Mode)	4 m
Range	67 m

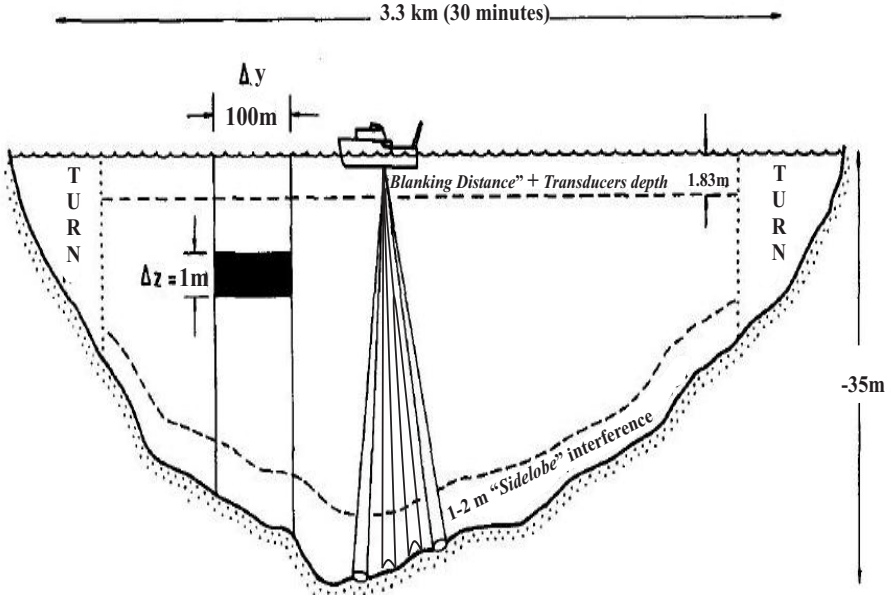

Fig. 2: Schematic of strategy for MV-ADCP measurements in which the boat repeatedly traversed the channel. There are no data available during turns at the end of each run and in near-surface and near-bottom sections of the profile.

Where u is representative of the component of horizontal velocity, u_0 the mean value of u over a tidal cycle, and for the nth constituent a_n is the amplitude, $\omega_n$the angular frequency, Φ_n phase angle, and t is time (Cáceres, Valle-Levinson et al. 2003). The root-mean-squared (rms) errors of the least-square fits were between ~ 0. 15 m/s and 0.38 m/s for the current transect and the mean error was about 0.13 m/s.

The 13 hour-period of the observation just allows us to resolve the semidiurnal tides. As mentioned before, KCh is dominated by semidiurnal tides anyway, then we will choose M_2 as one of the tidal frequencies in the harmonic analysis. Because of the short length of measurements, we are unable to distinguish between the different semidiurnal tides (e.g., N_2 and M_2). Therefore the semidiurnal tide selected (M_2) will represent all semidiurnal tides (Li, Blanton et al. 2004). Furthermore, because of the limited number of measurements (13 repetitions), we are restricted by the Nyquist frequency and will not be able to resolve higher frequency overtides and compound tides except for the M4 and M_6 (Parker 1991). (Aubrey and Speer 1985, Parker 1991).

4. Results and Discussion

In this part, we will represent the across-channel distribution of the mean and tidal flows in the KCh for the period of moving vessel ADCP surveys.

4.1. Moving Vessel -ADCP Surveys

4.1.1 Mean flow

Spatial distribution of u-mean flow (over a semidiurnal tidal cycle) showed it is strongly influenced by bathymetric variations. Results showed that outflows (positive values) occurred in the deeper part of the channel and southern slope and inflows (negative values) took place over the shallower areas, which was more evident in the southern side of the channel (Fig 3). The greatest magnitudes (10 cm/s) of the u-mean flow were observed near the surface mainly in the deeper parts of the northern side of the channel. The observed mean flow might be attributed to nonlinearities in the dynamics of tidal flow as pointed out by the theoretical results of (Li and O'Donnell 1997). They found that exchange flows were correlated with topography in such a way that mean inflows occurred over the shoals and out flows in the deeper parts of channel. The mean flow in the KCh also was resembled the mean flow in Chacao Channel, a highly energetic channel in Chile (Cáceres, Valle-Levinson et al. 2003) and also reminded the mean flow in North Inlet, a strongly frictional tidal channel in South Carolina, USA (Kjerfve and Proehl 1979) where the outflows occurs over the slopes and in the deeper part of the channel and inflows located over the shallower areas.

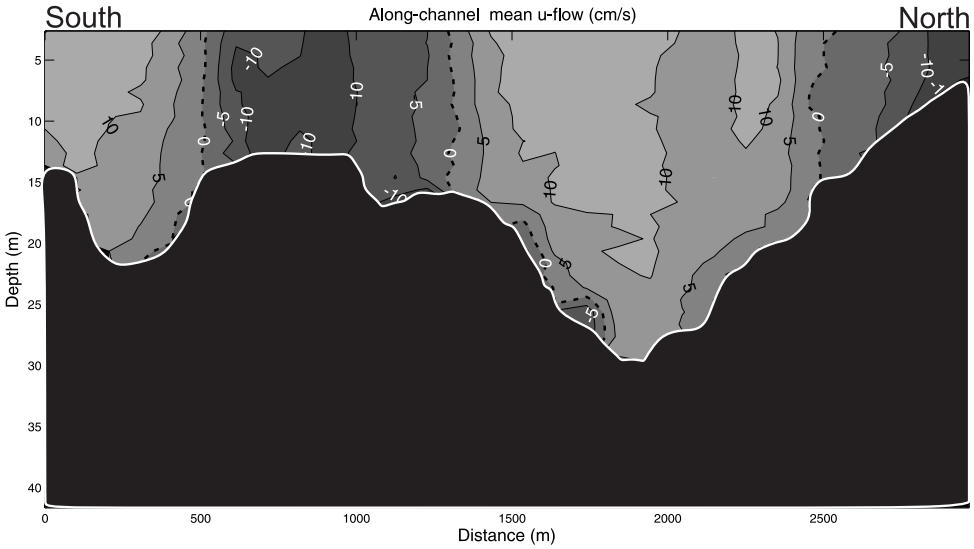

Fig. 3: Across-channel distributions of the u- mean flow

The vertical structure of the flow shows no strong shear (Fig. 4), and the weak vertical shear of the horizontal velocity is apparently caused by friction, not stratification, as also the study of (Zaker, Ghaffari et al. 2011) showed that the water column over most of the KCh is almost vertically homogenous. The mean flow in the KCh confirmed the occurrence of asymmetry between ebb and flood phase of tidal current.

In the case of spatial distribution of mean v-flow (Fig. 5), it featured no changes of direction near the surface. Therefore there was not any evidence of significant divergent or convergent area over the water column.

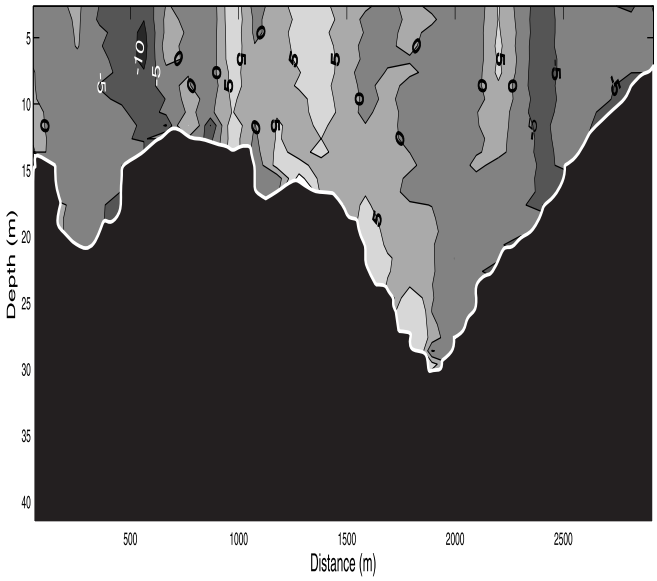

Fig. 4: Contours of the mean lateral shear $\left(\left(\frac{\partial \mathrm{u}}{\partial \mathrm{v}}\right) \times 10^{-4}\mathrm{S}^{-1}\right)$ of the u- flow

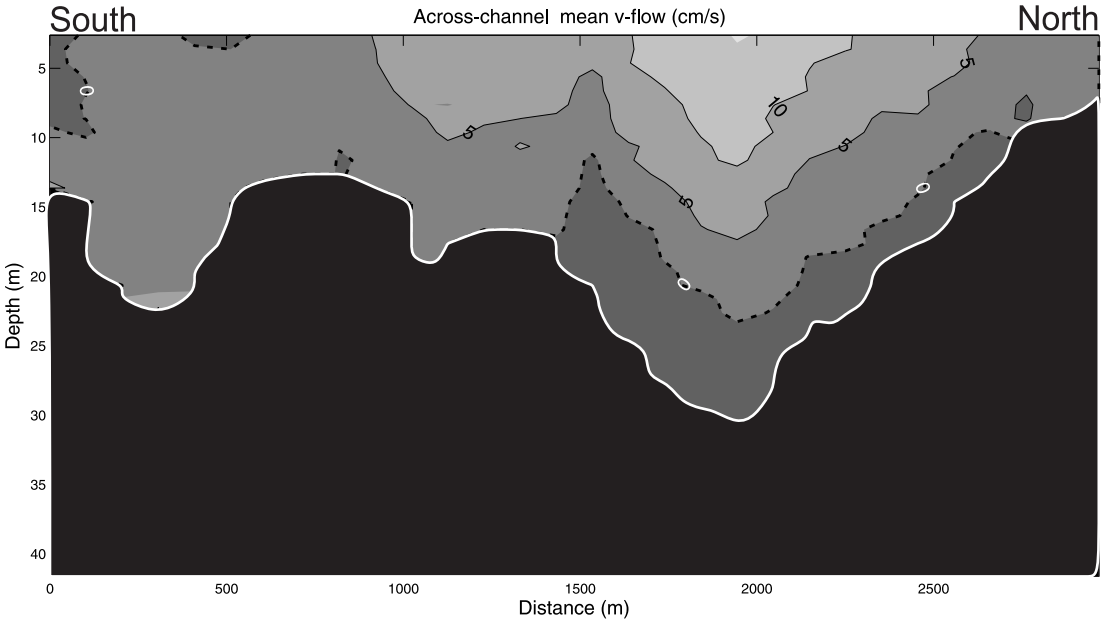

Fig. 5: Contours of the mean divergence $\left(\left(\frac{\partial \mathrm{v}}{\partial y}\right) \times 10^{-4}\mathrm{s}^{-1}\right)$ of the across-channel flow.

4.1.2 Tidal flow

Tidal flow in the KCh was mostly along the channel, dominated by semidiurnal signal. The across-channel distribution of the semidiurnal tidal current amplitudes is shown in Fig. 6. Highest amplitudes of about 160-170 cm/s occurred near surface in the mid channel. Generally, the semidiurnal signal decreased for the most with depth and followed the bathymetry, which reveals the dominants of frictional forces in agreement with (Parker 1991, Walters and Werner 1991, Friedrichs and Madsen 1992, Valle-Levinson and Lwiza 1995, Valle-Levinson and Lwiza 1997, Valle-Levinson and Atkinson 1999, Valle-Levinson, Wong et al. 2000, Cáceres, Valle-Levinson et al. 2003, Valle-Levinson, Reyes et al. 2003).

Tidal flow in the KCh also is slightly asymmetric such that velocity at maximum ebb was slightly larger than that at maximum flood at most places in agreement with (Blanton, Lin et al. 2002, Cáceres, Valle-Levinson et al. 2003). The u-mean flow discussed in the former section also confirmed this asymmetry.

Looking more closely at the spatial distribution of M2, M4 and M6 (Fig. 6, 7 and 8), it can be seen that their lateral variations were larger than their vertical variation. The regions of high values of the M4and M6 were almost extended over the water column in the mid channel. The large overtide amplitude might be a result of nonlinearities that were produced by increased frictional effects. In favor of this hypothesis, the greatest magnitudes of M6 in the mid channel confirm the influence of bottom frictional forces in agreement with those results of (Aubrey and Speer 1985, Parker 1991).

This was also concluded by M_2 contours which mostly followed the bathymetric contours. The large overtide amplitude which is mainly produced by the effect of frictional forces will generate an asymmetry between ebb and flood phase of tidal current and therefore lead to the observed mean flow over the period of observation.

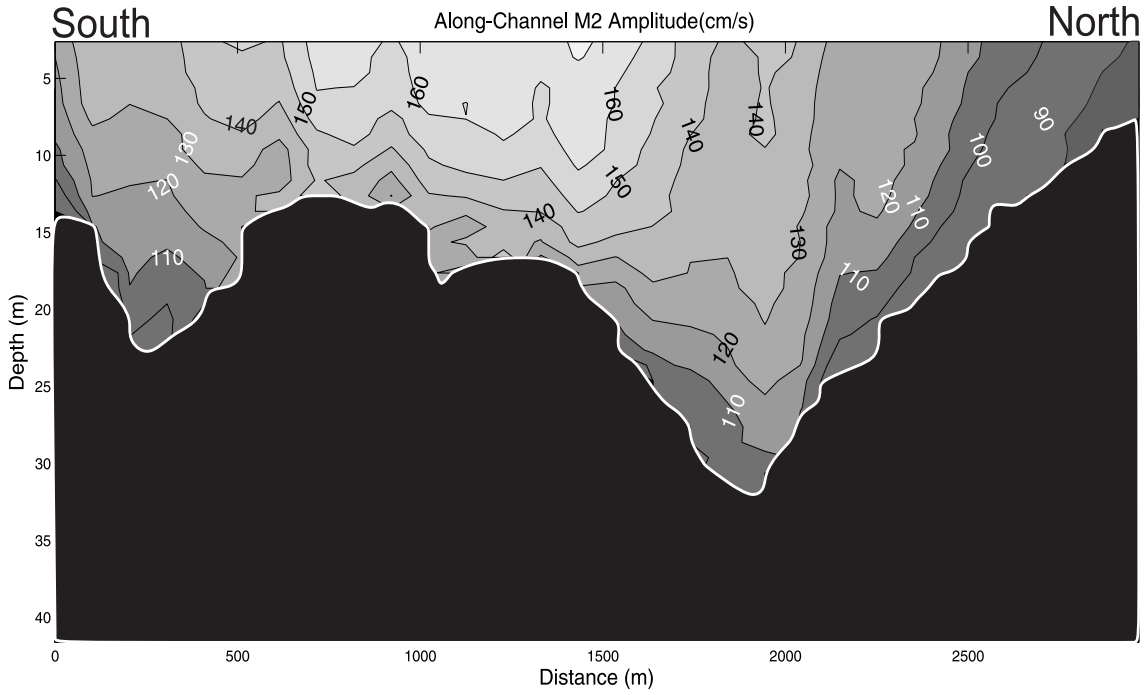

Fig. 6: Across-channel tidal amplitude distributions for the M2 constituent

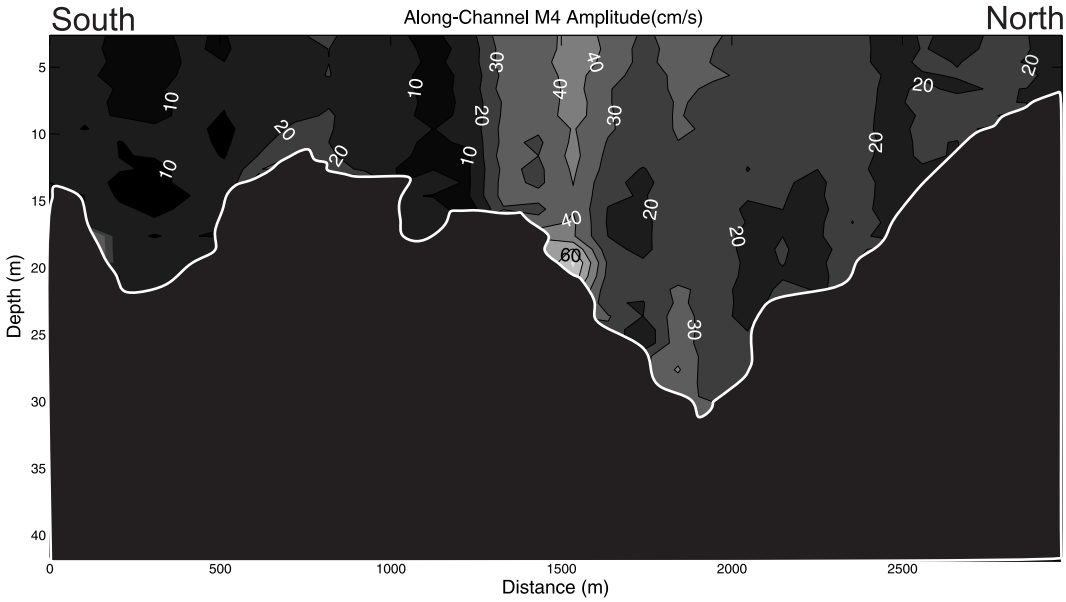

Fig. 7: Across-channel tidal amplitude distributions for the M4 constituent

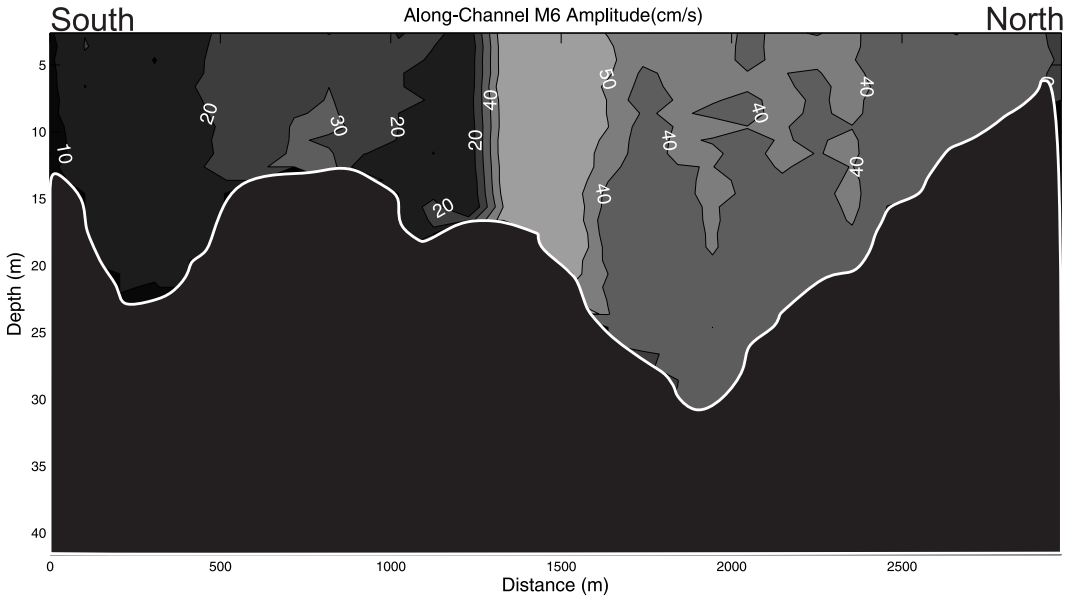

Fig. 8: Across-channel tidal amplitude distributions for the M6 constituent

5. Conclusions

This study has shown the capability of a moving vessel ADCP surveys in acquiring the spatial and temporal distribution of mean and tidal current in a greatly risky region (KCh) for the moored observation, since this area is exposed to the high volume of ship traffic as well as extensive fishing activities. Across-channel tidal amplitude distributions for the M2 constituent along this transect exhibited typical amplitudes of 160-170 cm/s, decreasing toward coastal waters. Over the period of observation, the mean flow were ebb dominant in the deeper part of the channel and southern slopes and flood dominant over the shallower areas, with greatest magnitudes (10 cm/s) near the surface mainly in the deeper parts of the northern side of the channel resemble to theoretical results of (Li and O'Donnell 1997) and observation of mean flow in Chacao Channel (Cáceres, Valle- Levinson et al. 2003) and also the

mean flow in North Inlet (Kjerfve and Proehl 1979).The mean flow confirmed the asymmetry between ebb and flood phase of tidal current in the KCh. The tidal current amplitudes decreased and for the most with depth and followed the bathymetry particularly in the mid channel, which reveals the dominants of frictional forces. The large overtide amplitude is as a consequence of nonlinearities that were produced by increased frictional effects that lead to the asymmetry between ebb and flood phase of tidal flow in the KCh.

References

Aubrey, D. and P. Speer, 1985. A study of non-linear tidal propagation in shallow inlet/estuarine systems Part I: Observations. Estuarine, Coastal and Shelf Science 21(2): 185-205.

Azizpour, J., S. M. Siadatmousavi and V. Chegini, 2016. Measurement of tidal and residual currents in the Strait of Hormuz. Estuarine, Coastal and Shelf Science.

Blanton, J. O., G. Lin and S. A. Elston, 2002. Tidal current asymmetry in shallow estuaries and tidal creeks. Continental Shelf Research 22(11): 1731-1743.

Buschman, F., 2017. Determining flow velocity near the bed in a scour hole using ADCP observations. Netherlands Centre for River Studies.

Cáceres, M., A. Valle-Levinson and L. Atkinson, 2003. Observations of cross□channel structure of flow in an energetic tidal channel. Journal of Geophysical Research: Oceans 108(C4).

Carpman, N. and M. Leijon, 2014. Measurements of tidal current velocities in the Folda Fjord, Norway, with the use of a vessel mounted ADCP. Proc. ASME.

Chen, Z., S. Wang and Z. Wang, 2016. A new interpolation scheme for detiding vessel-mounted ADCP data in tidal reach of Yangtze Estuary. Flow Measurement and Instrumentation 50: 185-196.

Friedrichs, C. T. and O. S. Madsen, 1992. Nonlinear diffusion of the tidal signal in frictionally dominated embayments. Journal of Geophysical Research: Oceans 97(C4): 5637-5650.

Geyer, W. R. and R. Signell, 1990. Measurements of tidal flow around a headland with a shipboard acoustic Doppler current profiler. Journal of Geophysical Research: Oceans 95(C3): 3189-3197.

Joyce, T. M., 1989. On in situ "calibration" of shipboard ADCPs." Journal of Atmospheric and Oceanic Technology 6(1): 169-172.

Kjerfve, B. and J. A. Proehl 1979. Velocity variability in a cross-section of a well-mixed estuary. Journal of Marine Research 37(3): 409-418.

Li, C., J. Blanton and C. Chen, 2004. Mapping of tide and tidal flow fields along a tidal channel with vessel-based observations. Journal of Geophysical Research: Oceans 109(C4).

Li, C. and J. O'Donnell, 1997. Tidally driven residual circulation in shallow estuaries with lateral depth variation. Journal of Geophysical Research: Oceans 102(C13): 27915-27929.

Lwiza, K., D. Bowers and J. Simpson, 1991. Residual and tidal flow at a tidal mixing front in the North Sea. Continental Shelf Research 11(11): 1379-1395.

Münchow, A., R. W. Garvine and T. F. Pfeiffer, 1992. Subtidal currents from a shipboard acoustic Doppler current profiler in tidally dominated waters. Continental Shelf Research 12(4): 499-515.

Old, C. and R. Vennell, 2001. Acoustic Doppler current profiler measurements of the velocity field of an ebb tidal jet. Journal of Geophysical Research: Oceans 106(C4): 7037-7049.

Parker, B. B., 1991. Tidal hydrodynamics, John Wiley & Sons. , New York, pp.237–268.

Reynolds, R. M., 1993. Physical oceanography of the Gulf, Strait of Hormuz, and the Gulf of Oman—Results from the Mt Mitchell expedition. Marine Pollution Bulletin 27: 35-59.

Valle-Levinson, A. and L. P. Atkinson, 1999. Spatial gradients in the flow over an estuarine channel." Estuaries 22(2): 179-193.

Valle-Levinson, A. and K. M. Lwiza, 1997. Bathymetric influences on the lower Chesapeake Bay hydrography. Journal of Marine Systems 12(1): 221-236.

Valle-Levinson, A., C. Reyes and R. Sanay, 2003. Effects of bathymetry, friction, and rotation on estuary-ocean exchange. Journal of Physical Oceanography 33(11): 2375-2393.

Valle-Levinson, A. and K. M. Lwiza, 1995. The effects of channels and shoals on exchange between the Chesapeake Bay and the adjacent

ocean. Journal of Geophysical Research: Oceans 100(C9): 18551-18563.

Valle-Levinson, A., K. C. Wong and K. M. Lwiza, 2000. Fortnightly variability in the transverse dynamics of a coastal plain estuary. Journal of Geophysical Research: Oceans 105(C2): 3413-3424.

Walters, R. A. and F. E. Werner, 1991. Nonlinear generation of overtides, compound tides, and residuals. Tidal hydrodynamics: 297-320.

Zaker, N., P. Ghaffari, S. Jamshidi and M. Nourian, 2011. Dynamics of the Currents in the Strait of Khuran in the Persian Gulf. Journal of Shipping and Ocean Engineering 1(2).